

Site-Specific Valence Determination by Electron Energy-Loss Spectroscopy

J. Taftø and O. L. Krivanek

Department of Physics and the Center for Solid State Science, Arizona State University, Tempe, Arizona 85287

(Received 18 December 1981)

The valence of an atom occupying a particular crystal lattice site can be determined from the chemical shift in a transmission electron energy-loss spectrum obtained with the intensity of the incident electron wave maximized at that site by dynamical electron diffraction. The new technique is demonstrated by determining the location of Fe^{2+} and Fe^{3+} ions in a mixed-valence spinel.

PACS numbers: 79.20.Kz, 71.70.Ms

Bragg reflection of a plane-wave incident on a crystal creates a standing-wave intensity pattern inside the crystal unit cell.¹⁻³ Depending on the orientation of the incident wave with respect to the crystal, the intensity maxima of this pattern will be located at the atomic sites or between them, or, in the case of more complex crystals, at one or another crystal site. If the incident radiation also produces characteristic ionization processes which are sufficiently localized,⁴ signals associated with the ionization will depend on the distribution of the standing-wave field inside the crystal unit cell. Several techniques based on this principle but employing different incident and emitted radiations have been developed. X rays have been used as both the primary and the emitted radiation (fluorescence) to identify the site of impurity atoms in a crystal matrix⁵ and to determine the distance of adsorbed atoms from a crystal surface.⁶ Electrons have been used as the primary radiation together with x rays as the emitted radiation to verify the existence of the modulated primary wave field⁷ and to determine the location of minority atoms,⁸ and together with energy analysis of the transmitted electrons to study the localization of the inner-shell ionization process for various light atoms.⁴ In this paper we show that by detecting the chemical shift in the energy-loss spectrum of the transmitted electrons as a function of incident beam direction, the valence of an atom occupying a particular crystal site may be determined.

A chromite spinel, $\text{Cr}_{1.1}\text{Fe}_{0.7}\text{Al}_{0.7}\text{Mg}_{0.5}\text{O}_4$, was studied. The location of the cations had been determined previously.⁸ Three quarters of the Fe atoms occupy tetrahedral sites and one quarter octahedral sites. Previous evidence indicated that the $\text{Fe}^{2+}:\text{Fe}^{3+}$ ratio is also 3:1, but the distribution of the Fe^{2+} and Fe^{3+} ions among octahedral and tetrahedral sites was not known. An ion-thinned specimen was examined in a Philips

400T transmission electron microscope equipped with a Gatan 607 magnetic sector electron energy-loss spectrometer.⁹ Areas about 1 μm in diameter in the thinnest regions of the specimen (thickness $\sim 500 \text{ \AA}$) were illuminated with 100-keV electrons. The incident beam was nearly parallel to the crystal (100) planes [$(h00)$ systematic orientation] and the beam divergence was up to 10 mrad (0.3 \AA^{-1}). The electrons selected for energy analysis were scattered by about 17 mrad and had an angular spread of also up to 10 mrad.

Along the $\langle 100 \rangle$ direction in a spinel, the octahedral-site atoms (all oxygen atoms and $\frac{2}{3}$ of cations) occupy one set of alternate (800) planes, and the tetrahedral-site atoms ($\frac{1}{3}$ of cations) occupy the other set midway between. The repetition distance is $d_{400} = 2.1 \text{ \AA}$. With the incident beam nearly perpendicular to $\langle 100 \rangle$ but away from any major zone axis (planar case), the standing-wave field in the crystal is largely determined by the more densely populated planes of octahedral-site atoms, while the less numerous tetrahedral-site atoms can be regarded as interstitials lying between octahedral planes, and having only a small effect on the standing-wave field. Two-beam dynamical theory then predicts⁴ that the incident-wave intensity maxima will be located at the octahedral planes when the incident beam angle with respect to the (400) planes is just less than the Bragg angle [incident beam appears within the (400) Kikuchi band], and at the tetrahedral planes when the incident beam angle to the (400) planes is just greater than the Bragg angle [incident beam outside the (400) Kikuchi band]. As in our previous experiments,⁴ we enhanced the site selectivity by choosing the direction of the scattered (collected) beam to be the same with respect to the (400) planes as the direction of the incident beam. In this scattering geometry the outgoing wave diffracts in much the same way as the incident wave¹⁰ when time reversal is considered (prin-

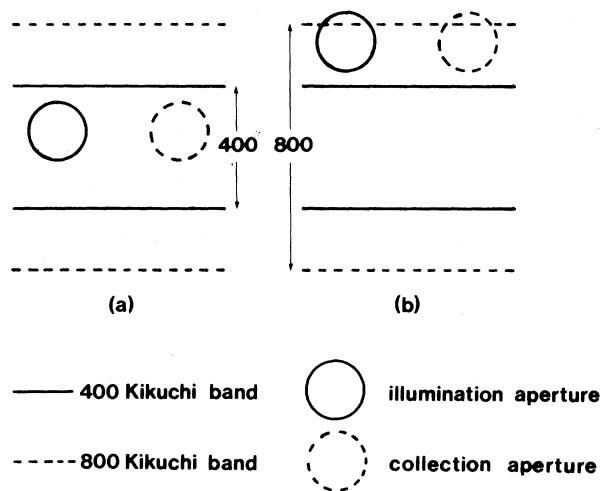


FIG. 1. Diffraction geometries used to set up standing-wave fields with maxima at different sites. (a) Octahedral sites selected and (b) tetrahedral sites selected. Note that the $(h00)$ Bragg condition is satisfied exactly at the corresponding $(h00)$ Kikuchi line.

principle of reciprocity), and the site selectivity is enhanced in a similar way to double alignment in particle channeling.¹¹ We then further maximized the site selectivity by choosing a fairly large (~ 17 mrad) scattering angle parallel to the (400) Kikuchi band such that only ionization events due to electrons passing within ~ 1 Å of the atomic nucleus were registered (localization enhancement). The scattering arrangement is illustrated schematically in Fig. 1. In the actual experiment the diffraction pattern was displayed on a removable screen in front of the spectrometer entrance aperture, and the scattering conditions were adjusted by tilting the crystal in a double tilt holder and by using post-specimen beam deflector coils.

Figure 2 shows electron energy-loss spectra acquired in 200 sec under each of the conditions illustrated in Fig. 1. Oxygen K edge (all atoms on octahedral sites), Cr $L_{2,3}$ edge (all atoms on octahedral sites), and Fe $L_{2,3}$ edge ($\frac{3}{4}$ on tetrahedral sites, $\frac{1}{4}$ on octahedral sites) are displayed. With both the incident and collected beams inside the (400) band the O and Cr edges predominate, whereas in the "outside geometry" the O and Cr edges are diminished while the Fe $L_{2,3}$ edge becomes stronger. This establishes that selective enhancement of the signal from the two different sites has indeed been obtained. It also agrees with the previous determination of Cr and Fe lattice sites,⁸ as can be seen simply by contrasting the change in the intensity of the Cr and Fe

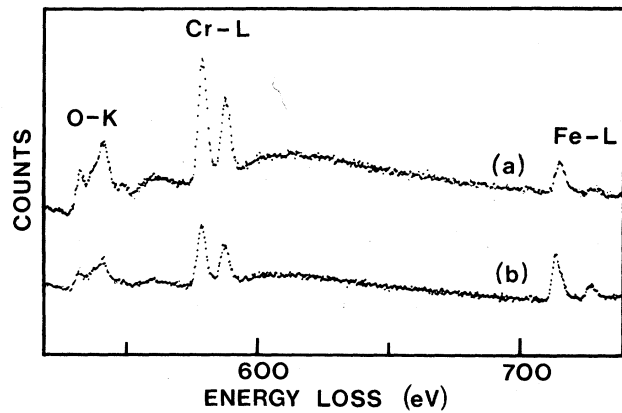


FIG. 2. Electron energy-loss spectra of chromite spinel taken under the two conditions illustrated in Fig. 1.

edges with the change in the oxygen edge.

Figure 3 shows the detail of the Fe $L_{2,3}$ edge in spectra acquired separately in 50 sec each. The sharp peaks at the edge threshold, due to the transition of the $2p$ electrons to a high concentration of empty d states just above the conduction-band edge, are split into two components separated by 2 eV. Such splitting has not been observed in any single-valence iron compound, but it is consistent with a 2 eV chemical shift between Fe^{2+} and Fe^{3+} , with the Fe^{3+} peak at the higher energy according to the usual relationship between the chemical shift and the valence state.¹² The strength of the higher-energy component varies in the same way as the strength of the oxygen and chromium edges, while the dominant lower-energy component varies in the

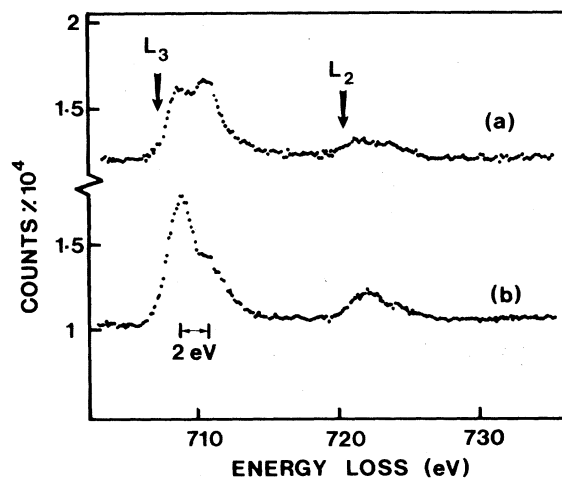


FIG. 3. Detail of the iron $L_{2,3}$ edge in chromite.

opposite way. Thus we attribute the lower-energy peak to Fe ions occupying the tetrahedral sites and the higher-energy peak to Fe ions occupying the octahedral sites, and conclude that the tetrahedral sites hold Fe^{2+} ions and the octahedral sites hold Fe^{3+} ions. This completes the previous analysis of this chromite,⁸ showing it to be a normal spinel in all aspects (3+ valence cations on octahedral sites and 2+ valence cations on tetrahedral sites).

To verify that the observed chemical shift is mostly due to a change in valence and not just due to the different sites, we have also investigated ilmenite ($\text{Ti}^{4+}\text{Fe}^{2+}\text{O}_3$, octahedral iron), hematite ($\text{Fe}_2^{3+}\text{O}_3$, octahedral iron), and magnetite (Fe_3O_4 ; octahedral Fe^{3+} , octahedral Fe^{2+} , and tetrahedral Fe^{3+} in equal proportions). The $\text{Fe}^{3+} L_3$ threshold peak in hematite was 1.3 ± 0.3 eV higher in energy than the $\text{Fe}^{2+} L_3$ peak in ilmenite. This indicates that a larger part of the 2-eV shift observed in chromite is due to the change in valence, but that ~ 0.7 eV may be due to the change in site. In magnetite we observed a broadening of the L_3 threshold peak when the octahedral sites were selected as opposed to the tetrahedral sites. This was expected since the octahedral signal comes from Fe^{3+} and Fe^{2+} and should therefore consist of two L_3 threshold peaks separated by about 1.3 eV, while the tetrahedral signal comes from Fe^{3+} alone and should therefore consist of a single L_3 peak about halfway between the first two. The broadening in the octahedral case was only ~ 0.5 eV and the two peaks were not resolved, but this is consistent with the finite instrumental resolution (~ 1 eV), finite L_3 linewidth (~ 2 eV), and the fact that a small tetrahedral signal remains even when the octahedral-selecting scattering geometry is employed and vice versa. We summarize by noting that care must be exercised in any future determination of site valence to separate the valence-dependent and the site-dependent chemical shifts. With suitable standards in which the valence change and the site change effects exist separately, however, differentiating between the two types of shift should be possible.

Another interesting observation is that in Fig. 3(a), the higher-energy L_3 -threshold-peak component rises above the lower-energy component, while for the L_2 threshold peak the reverse is the case. This is consistent with a previously observed increase¹³ in the iron $L_3:L_2$ white line ratio with increased oxidation state. It provides additional support for assigning the lower-energy

peaks to Fe^{2+} and the higher-energy peaks to Fe^{3+} , and hence also for the finding that the Fe^{2+} atoms occupy tetrahedral sites and the Fe^{3+} atoms occupy octahedral sites.

We note that our new method is only one of a variety of related methods which should all be capable of site-specific valence determination. For instance, x rays or particles under channeling conditions could be used as the primary beam, and x-ray absorption, x-ray fluorescence, photoelectrons, or Auger electrons as the detected signal. The applicability of the method will be limited to crystals in which it is possible to set up diffraction conditions that maximize the incident wave intensity at the crystal sites of interest, and in which the chemical shift is about 1 eV or greater at present, but probably much less in the future with improved instrumentation. In contrast to Mössbauer spectroscopy, our method is not limited to certain elements or low temperatures, and should therefore prove useful on the many outstanding site valence determination problems.

We are grateful to the National Science Foundation (Grants No. DMR8002108 and No. CHE-7916098) and the Arizona State University HREM facility for financial support, the Smithsonian Institution, Washington, D. C., for supply of the chromite (Museum No. 112997, locality Stillwater Complex, Montana), J. Smyth for discussions and supply of test specimens, and to J. C. H. Spence for his enthusiastic interest in this work.

¹G. Borrmann, *Phys. Z.* **42**, 157 (1941).

²P. B. Hirsch, A. Howie, and M. J. Whelan, *Philos. Mag.* **7**, 2095 (1962).

³B. W. Batterman, *Phys. Rev.* **133**, A759 (1964).

⁴J. Taftø and O. L. Krivanek, to be published; O. L. Krivanek, J. Taftø, and J. C. H. Spence, unpublished results.

⁵B. W. Batterman, *Phys. Rev. Lett.* **22**, 703 (1969).

⁶P. L. Cowan, J. A. Golovchenko, and M. F. Robbins, *Phys. Rev. Lett.* **44**, 1680 (1980).

⁷P. Duncumb, *Philos. Mag.* **7**, 2101 (1962).

⁸J. Taftø, to be published.

⁹O. L. Krivanek and P. R. Swann, in *Proceedings of the Conference on Quantitative Microanalysis with High Spatial Resolution*, edited by M. Loretto (Arrowsmith, Bristol, 1981), p. 262.

¹⁰G. Lehmpfuhl and J. Taftø, in *Proceedings of the Seventh European Conference on Electron Microscopy*, edited by P. Brederoo and V. E. Cosslett (Electron Microscopy Foundation, Leiden, 1980), Vol. 3, p. 62; J. Taftø and O. L. Krivanek, in *Proceedings of the 39th*

Electron Microscopy Society of America Meeting, edited by G. W. Bailey (Claitor's, Baton Rouge, 1981), p. 190.

¹¹S. T. Picraux, W. L. Brown, and W. M. Gibson, *Phys. Rev. B* **6**, 1382 (1972).

¹²B. K. Agarwal, *X-ray Spectroscopy* (Springer-Verlag, Berlin, 1979), pp. 285-288.

¹³L. A. Grunes, in *Proceedings of the 38th Electron Microscopy Society of America Meeting*, edited by G. W. Bailey (Claitor's, Baton Rouge, 1980), p. 122.

High-Resolution Laser-Pulse Method for Measuring Charge Distributions in Dielectrics

G. M. Sessler,^(a) J. E. West, and G. Gerhard^(a)

Bell Laboratories, Murray Hill, New Jersey 07974

(Received 13 November 1981)

A laser-induced pressure-pulse method for measuring the charge distribution in (10 to 100 μm thick) dielectric samples with a resolution of about 4 μm is described. A short (< 1 ns) energetic light pulse from a neodymium-doped yttrium aluminum garnet laser is applied to a specially coated surface of the sample. The recoil due to ablation of material from the coating generates a pressure pulse (~ 2 ns) which propagates through the sample. The charge distribution is evaluated by measuring the electrode currents from 25- and 75- μm polymers charged with corona and electron-beam methods.

PACS numbers: 72.20.Jv, 41.10.Fs, 72.50.+b

During the past few years a number of methods to investigate charge distributions in dielectrics have been developed.¹ While the centroid can be conveniently measured with the thermal-pulse method,² it is more difficult to obtain detailed information about the actual distribution of the charge. Recently, however, progress has been made with two measuring techniques, namely the acoustic method³⁻⁶ and the electron-beam method.⁷⁻⁹

Existing acoustic methods use either a shock tube,³ a spark gap,⁴ or a ruby laser⁵ to excite pressure pulses or steps of about 0.1 μs duration, or a quartz crystal⁶ to generate a pressure step of about 1-ns risetime. The present acoustic method utilizes a very short laser-induced pressure pulse (LIPP) and differs in three important respects from the existing techniques: (1) The duration of LIPP is only about 1 ns which leads to high resolution without further signal processing; (2) the coupling of the LIPP into the sample is achieved directly without parallel-mounting or bonding problems; and (3) the LIPP technique is used not only for two-sided, but also for one-sided metalized samples.

The light pulses were generated by a mode-locked and Q-switched 1.064- μm neodymium-doped yttrium aluminum garnet (Nd:YAlG) laser¹⁰ system which allows a single-pulse operation. The length of the light pulses can be varied within the range of 70 to 1200 ps and the energy of a sin-

gle pulse can be chosen as high as 100 mJ, corresponding to a peak power of 1.4 GW. For most of the measurements, pulse energy of 50 mJ was used. The cross-sectional area of the beam at the sample surface was about 0.2 cm^2 .

The surface of the sample was mechanically excited by the laser pulse causing ablation of a graphite layer deposited on the sample surface prior to the experiment. The emission of the material generates a recoil which launches the desired pressure pulse. For a laser pulse of 70-ps duration, the beam intensity of 3.5 GW/cm^2 is sufficient to cause ablation.¹¹ The effect of the heat diffusion into the sample is beyond the time scale of the present experiment.

The LIPP of duration τ propagates with the velocity of sound c through the sample, as illustrated in Fig. 1. It is assumed that the length $c\tau$ of the LIPP is smaller than any characteristic length describing changes in the charge distribution of the sample. In an open-circuit arrangement of the sample electrodes, the pulse yields, for pressures not exceeding the elastic limit of the dielectric, a voltage response $V(t)$ given by⁴

$$V(t) = -(2 - \epsilon^{-1})\chi P c \tau E(ct), \quad (1)$$

where χ is the compressibility of the sample, P is the pressure amplitude of the pulse, and $E(ct) = E(x)$ is the local electric field in the sample.

Differentiation of Eq. (1) with respect to time and use of Poisson's equation $\epsilon \epsilon_0 dE/dx = \rho(x)$ with